

## Supporting Information:

### **An active and stable Ni/Al<sub>2</sub>O<sub>3</sub> nanosheet catalyst for dry reforming of CH<sub>4</sub>**

Lin Zhang and Yi Zhang \*

State Key Laboratory of Organic-Inorganic Composites; Research Centre of the Ministry of  
Education for High Gravity Engineering and Technology; Beijing University of Chemical  
Technology, Beijing 100029, China

\*Corresponding author: yizhang@mail.buct.edu.cn

## Contents

**SI-1.** Experimental details.

**SI-2.** Figure S1 TEM images of catalyst at different stage of experiments.

**SI-3.** Figure S2 XRD patterns of catalysts: (a) fresh, (b) passivated.

**SI-4.** Figure S3 H<sub>2</sub>-TPR profiles of the samples.

**SI-5.** Figure S4 TEM image of Ni/Al<sub>2</sub>O<sub>3</sub> (T) after 50 h reaction.

**SI-6.** Figure S5 TG / DTA profiles of Ni/Al<sub>2</sub>O<sub>3</sub> (T) after 50 h reaction.

**SI-7.** Figure S6 XRD patterns of used samples.

**SI-8.** Figure S7 TG / DTA profiles of used catalysts.

**SI-9.** Table S1 Textural and structural characteristics of the synthesized samples.

**References**

## SI-1. Experimental details

### Catalyst Preparation

Nickel 2, 4-pentanedionate and  $\text{Al}(\text{NO}_3)_3 \cdot 9\text{H}_2\text{O}$  was used as nickel source and aluminum source respectively. Moreover,  $(\text{NH}_2)_2\text{CO}$  and TX-100 were used as alkali source and surfactant respectively. All chemicals were of analytical grade and used without further re-purification. Nickel 2, 4-pentanedionate (0.46g) was dissolved in deionized water (70 mL), and then  $(\text{NH}_2)_2\text{CO}$  (0.11g) and Triton X-100 (0.05g) were added to form a clear solution under stirring at 333K. The reactant mixture was then transferred into a 150 mL Teflon-lined autoclave and heated at 423K for 2 h. After the autoclave had been allowed to cool to room temperature, the  $\text{Ni}(\text{OH})_2$  nanoparticles were re-dispersed by ultrasonic treatment and then  $\text{Al}(\text{NO}_3)_3 \cdot 9\text{H}_2\text{O}$  (6.62g),  $(\text{NH}_2)_2\text{CO}$  (1.67g) were added to this solution in order. The mixture was then transferred into a 150 mL Teflon-lined autoclave and heated at 423K for 5 h. When the reaction was completed, the autoclave was cooled to room temperature. The products were collected and purified by repeated centrifugation and then dried at 393 K for 2 h. Calcination step was carried out by slowly increasing temperature from room temperature to 773 K (2 K/min) and keeping at 773 K for 3 h. The as-prepared sample  $\text{Ni}/\text{Al}_2\text{O}_3$  was signed as fresh  $\text{Ni}/\text{Al}_2\text{O}_3$  (T). The  $\text{Ni}/\text{Al}_2\text{O}_3$  catalysts by one-step hydrothermal (signed as  $\text{Ni}/\text{Al}_2\text{O}_3$  (O)) used a 150 mL Teflon-lined autoclave and heated at 423K for 5 h. For comparison, a conventional  $\text{Ni}/\text{Al}_2\text{O}_3$  catalyst was prepared by impregnation method (signed as  $\text{Ni}/\text{Al}_2\text{O}_3$  (I)) using  $\text{Al}_2\text{O}_3$  support synthesized by hydrothermal method under the same reaction conditions. The nickel loading of all catalysts was 10 wt %, which was confirmed by EDX.

### Characterization of catalysts

For characterization of reduced catalysts, the calcined catalysts were reduced by pure hydrogen at 1073 K for 2 h and then passivated by 1%  $\text{O}_2$  in  $\text{N}_2$  to form a metal oxide layer on the surface of metal particle in order to preventing oxidation of nickel metal when the catalysts were exposed to air.

The surface area and the pore size distribution were determined via nitrogen adsorption, using AUTOSORB-IQ instrument. The surface area was calculated using the BET method, while the pore size distribution curve was obtained from the adsorption branch of the N<sub>2</sub> isotherm by the BJH method.

XRD patterns of Ni/Al<sub>2</sub>O<sub>3</sub> catalysts were recorded on a D/Max 2500VB2+/PC diffractometer with Cu K $\alpha$  radiation ( $\lambda = 0.154056$  nm). The samples were scanned with a speed of 2 degree/min.

For the reduction behavior, temperature-programmed reduction (TPR) was carried out in a quartz tube reactor using 0.1 g calcined catalysts. The reducing gas, a mixture of 10% H<sub>2</sub> diluted by Ar, was fed via a mass flow controller at 30 cm<sup>3</sup>/min and then the sample was heated to 1173 K at a constant heating rate of 10 K/min. The signal of hydrogen consumption was detected by a thermal conduction detector (TCD). The effluent of reactor passed through a 5 A molecular sieve trap to remove produced water, before reaching TCD.

Scanning electron microscopy (SEM) was used to determine the catalyst granule morphology, using a JEOL JSM-7600F scanning electron microscope.

Thermo gravimetric thermal analysis (TG-DTA) was carried on a HTG-1 (henven) instrument from 323 K and 1073 K at a heating rate of 10 K/min to determine the carbon deposition of used catalysts.

Transmission electron microscopy (TEM) and High-resolution transmission electron microscopy (HRTEM) images of the catalysts were determined by JEM-2100 microscope. The specimen was prepared by ultrasonically suspending the catalyst powder in ethanol. A drop of the suspension was deposited on a carbon grid and dried in air.

Scanning transmission electron microscopy (STEM) was carried on a Tecnai G2 F20 S-TWIN instrument. The specimen was prepared in a similar way adopted in TEM characterization.

In order to study the thickness of Ni/Al<sub>2</sub>O<sub>3</sub> (T) catalyst, Atomic force microscopy (AFM) observations were performed by a DMFASTSCAN2-SYS instrument.

### **Catalysts testing in dry reforming of CH<sub>4</sub>**

The catalytic activity in CO<sub>2</sub> reforming of CH<sub>4</sub> was tested using a quartz tube reactor (7 mm in diameter) at atmospheric pressure. The 100 mg catalysts were loaded into reactor and reduced by hydrogen at 1073 K for 2h and then purged by N<sub>2</sub>. The dry reforming of methane reaction was carried out at 973 K or 1073 K under atmospheric pressure (Ar/CH<sub>4</sub>/CO<sub>2</sub>=4/48/48, where Ar is inner reference, GHSV=21000cm<sup>3</sup>·g<sup>-1</sup>·h<sup>-1</sup>). The products were analyzed by on-line gas chromatograph equipped with a thermal conductivity detector (TCD).

**SI-2.** Figure S1 TEM images of catalyst at different stage of experiments and XRD pattern of products of first step hydrothermal process

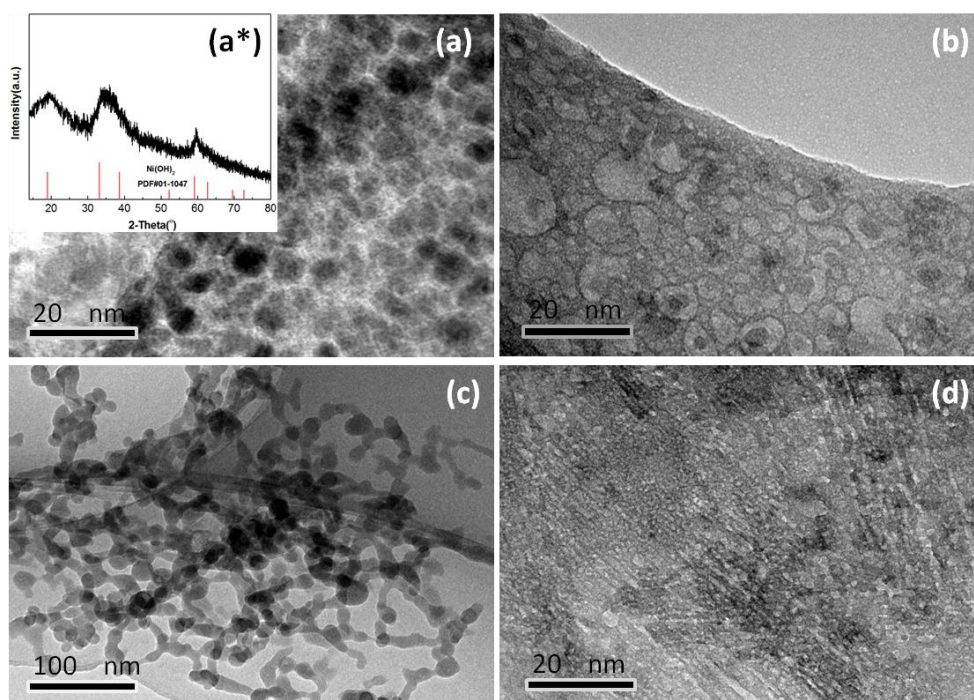
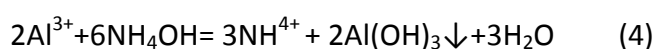
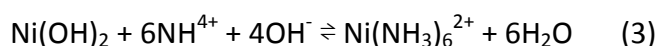
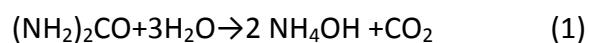


Fig.S1 TEM images of catalyst at different stage of experiments: (a) after the first step hydrothermal, (b) second step hydrothermal for 1h, (c) second step hydrothermal for 2h, (d) second step hydrothermal for 3h, (a\*)XRD pattern of products of first step hydrothermal process.

For the formation of leaf like nano structured Ni/Al<sub>2</sub>O<sub>3</sub> (T) catalyst, it is considered that the Ni(OH)<sub>2</sub> particles would partially dissolved into the solution of second hydrothermal reaction, leading to modifying the crystallization of Al<sub>2</sub>O<sub>3</sub>. As reported by Msharrafieh and Langer,<sup>1, 2</sup> the possible chemical reactions during secondary hydrothermal reaction could be presented as eq. (1)–(4).



Under the secondary hydrothermal conditions, the Ni(OH)<sub>2</sub> nanoparticles were gradually dissolved to generate Ni(NH<sub>3</sub>)<sub>6</sub><sup>2+</sup> and reacted with the Al(OH)<sub>3</sub> or AlOOH,

resulting in that redissolved  $\text{Ni}(\text{OH})_2$  entered the lattice of generated  $\text{Al}(\text{OH})_3$  or co-precipitated with the  $\text{Al}(\text{OH})_3$ .

Figure S1 exhibited the TEM images of  $\text{Ni}(\text{OH})_2$  particles after the first step hydrothermal process and products of secondary hydrothermal reaction at 423 K for 1 h, 2 h, and 3 h, respectively. The image of  $\text{Ni}(\text{OH})_2$  particles synthesized in the first step hydrothermal process (Fig. S1a) showed that the particles dispersed very well and diameters of the sphere-like particles were about 5 nm. As shown in Fig. S1a\*, the peaks attributed to  $\text{Ni}(\text{OH})_2$  (PDF#01-1047) were observed for the product of first step hydrothermal process. After 1h reaction of the second hydrothermal process, partial dissolution of  $\text{Ni}(\text{OH})_2$  particles and generation of  $\text{Al}(\text{OH})_3$  or  $\text{AlOOH}$  were observed as shown in Figure S1b. With increasing reaction time, it can be found that three or more particles are linked together each other at the certain principle in Fig. S1c. After 3h reaction (Fig. S1d),  $\text{Ni}(\text{OH})_2$  particles highly dispersed on  $\text{Al}(\text{OH})_3$  or  $\text{AlOOH}$  and the diameter of  $\text{Ni}(\text{OH})_2$  particles decreased to only about 2 nm, which is much smaller than that of  $\text{Ni}(\text{OH})_2$  particles formed in the first step hydrothermal process.

In recent years, the oriented attachment (OA) growth of crystals<sup>3</sup> has shown great potential in controlling and designing materials of various nanostructures. The structure is grown from small primary nanoparticles through an oriented attachment mechanism, in which the adjacent nanoparticles are self-assembled by sharing a common crystallographic orientation and docking of these particles at a planar interface. It is reported that the CuO nanoleaves<sup>4</sup> and well-defined CuO nano architectures<sup>5</sup> have been synthesized based on the OA growth of crystal. Therefore, it is considered that the leaf like nanosheet of  $\text{Ni}/\text{Al}_2\text{O}_3$  (T) catalyst (Fig. 2a) might be formed following the oriented attachment (OA) growth of crystals.

SI-3. Figure S2 XRD patterns of catalysts: (a) fresh, (b) passivated.

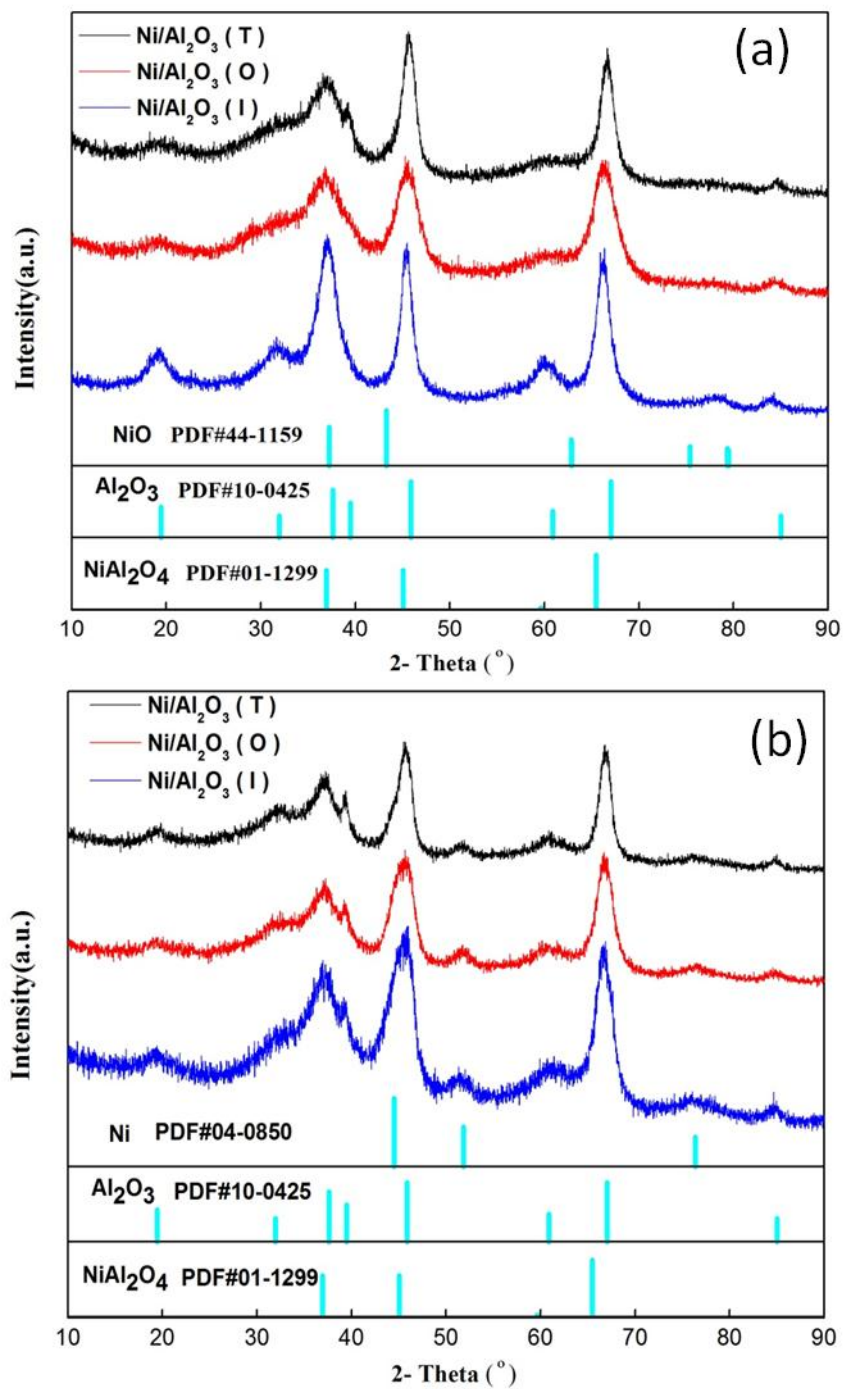


Fig.S2 XRD patterns of catalysts: (a) fresh, (b) passivated



SI-4. Figure S3 H<sub>2</sub>-TPR profiles of the samples.

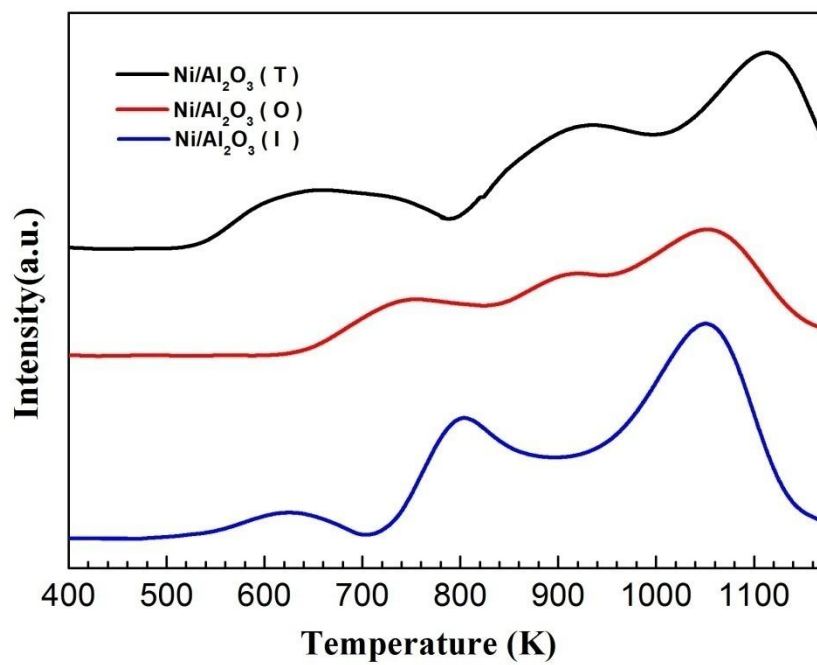


Fig. S3 H<sub>2</sub>-TPR profiles of three catalysts.

SI-5. Figure S4 TEM image of Ni/Al<sub>2</sub>O<sub>3</sub>(T) after 50 h reaction.

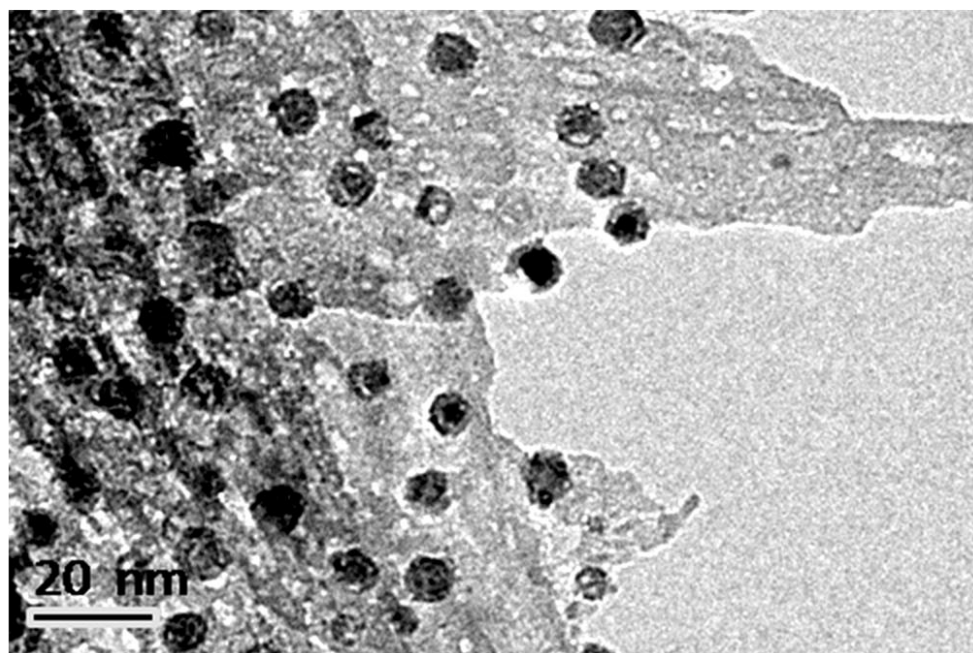


Fig. S4 TEM image of Ni/Al<sub>2</sub>O<sub>3</sub>(T) after 50 h reaction.

SI-6. Figure S5 TG/DTA profiles of Ni/Al<sub>2</sub>O<sub>3</sub> (T) after 50 h reaction.

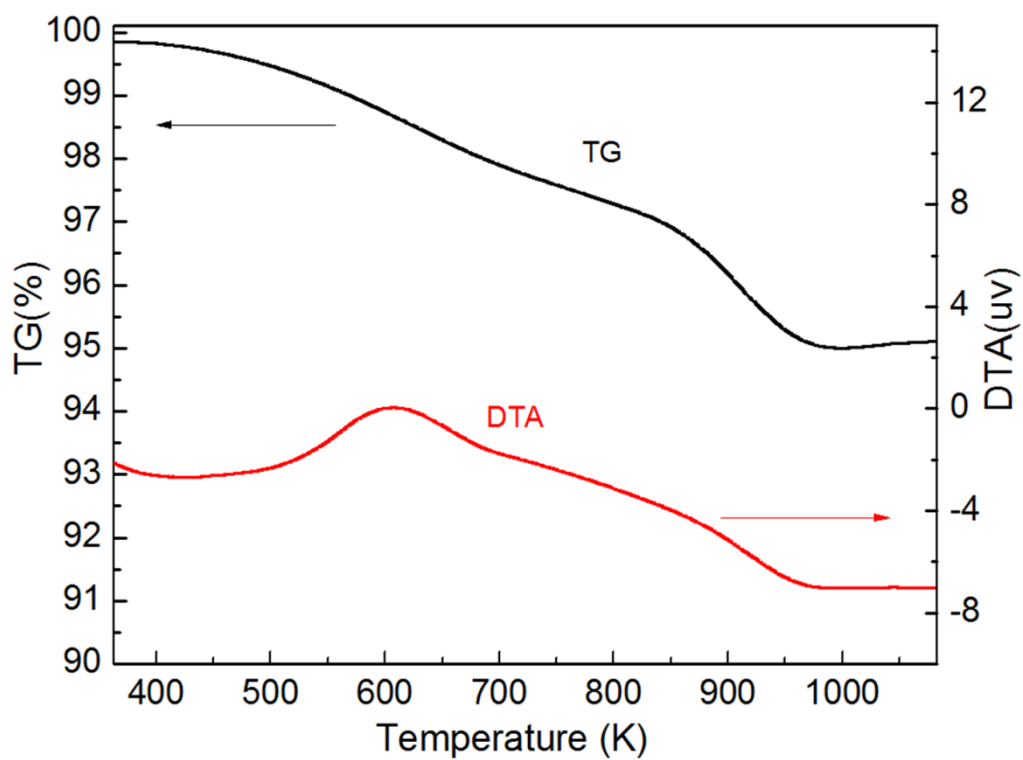


Fig. S5 TG/DTA profiles of Ni/Al<sub>2</sub>O<sub>3</sub> (T) after 50 h reaction.

SI-7. Figure S6 XRD patterns of used catalysts

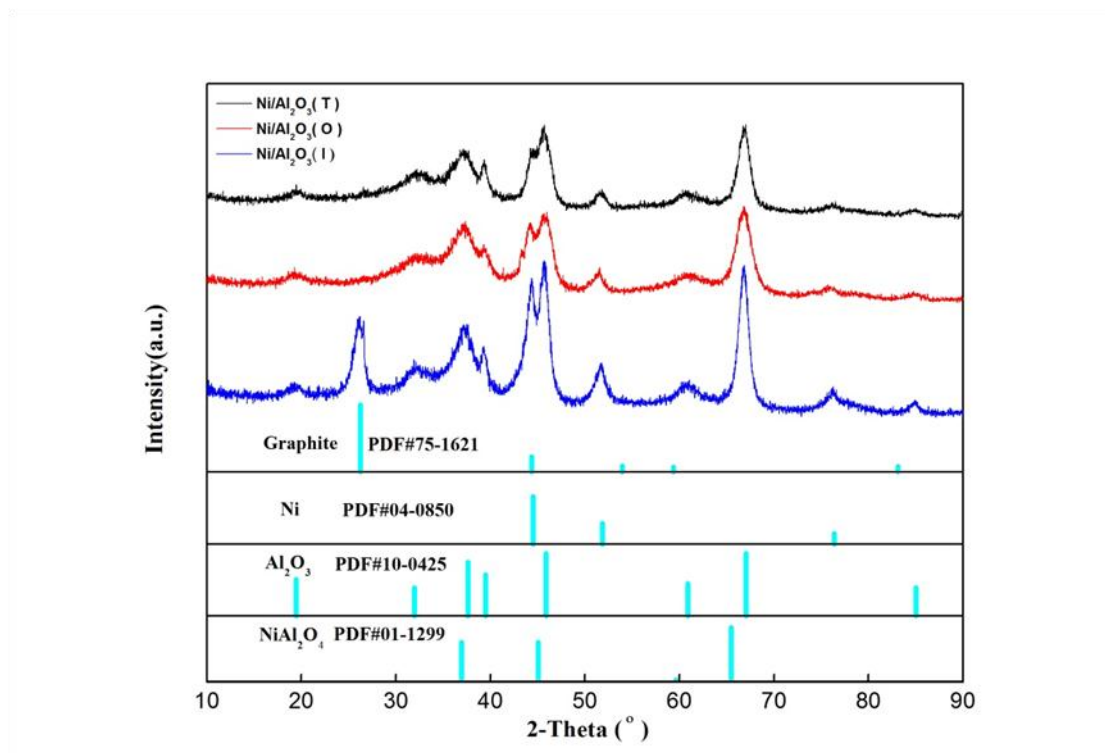


Fig. S6 XRD patterns of used catalysts

SI-8. Figure S7 TG / DTA profiles of used catalysts.

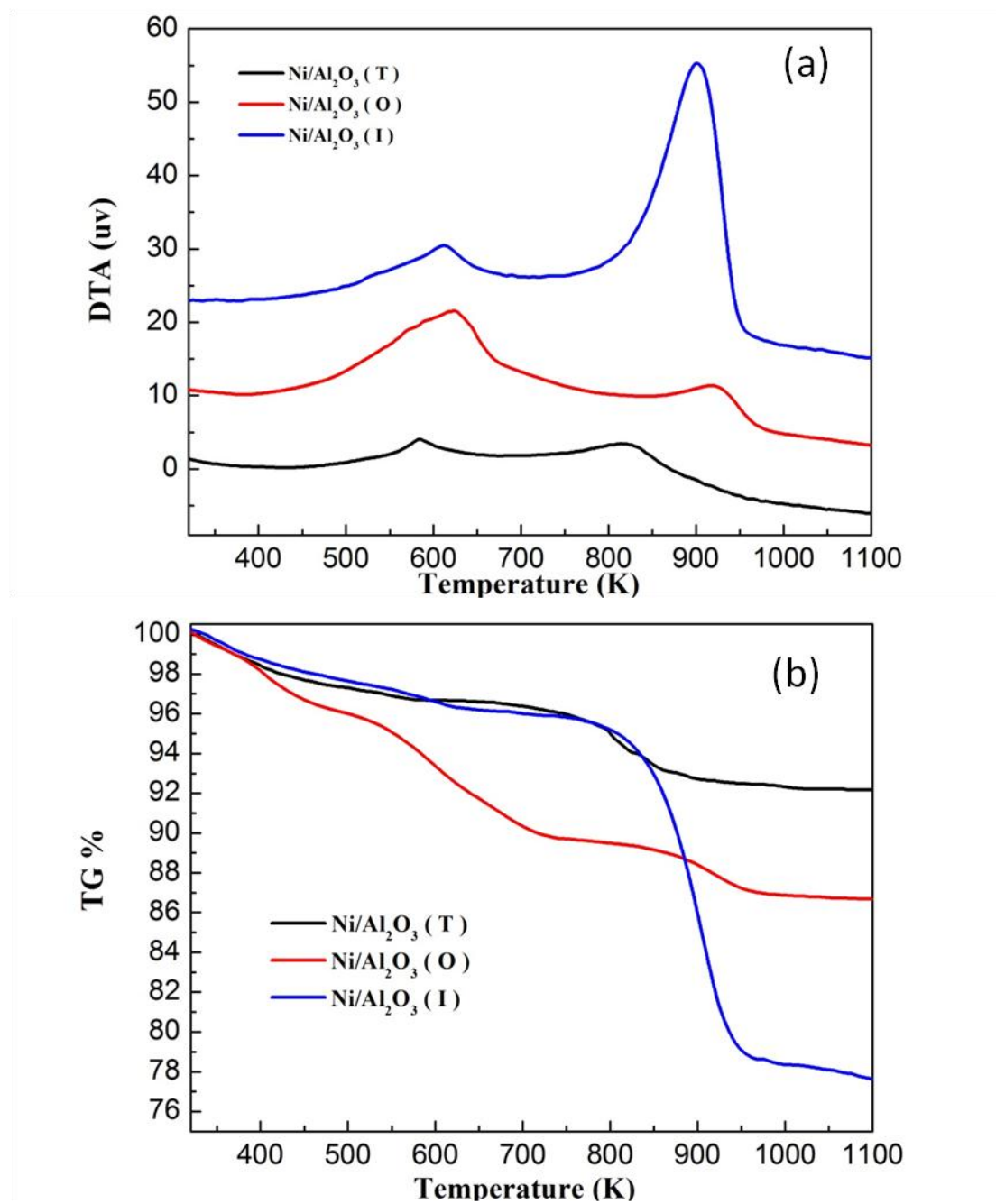


Fig. S7 TG / DTA profiles of used catalysts after CO<sub>2</sub>/CH<sub>4</sub> reforming at 973 K for 10 h.

**SI-9.** Table S1 Textural and structural characteristics of the synthesized samples.

**Table S1** Physiochemical properties of various catalysts.

Catalysts	$S_{\text{BET}}$ ( $\text{m}^2/\text{g}$ ) <sup>a</sup>	Pore volume ( $\text{cc/g}$ ) <sup>b</sup>	Pore size ( $\text{nm}$ ) <sup>b</sup>	Ni cluster size ( $\text{nm}$ ) <sup>c</sup>		Ni particle size ( $\text{nm}$ ) <sup>c</sup>	
				passivated	used	passivated	used
Ni/Al <sub>2</sub> O <sub>3</sub> (T)	508	0.64	2.4	9.62	9.78	2.15	2.21
Ni/Al <sub>2</sub> O <sub>3</sub> (O)	141	0.22	2.9	6.81	8.14	1.81	2.32
Ni/Al <sub>2</sub> O <sub>3</sub> (I)	258	0.59	6.1	8.02	12.15	2.32	3.84

<sup>a</sup> BET surface area; <sup>b</sup> Calculated by BJH method; <sup>c</sup> Average cluster size calculated from TEM images.

## References

- 1 M. Msharrafieh, M. Al-Ghoul, *J. Phys. Chem. A*, 2007, **111**, 6967–6976.
- 2 J. S. Langer, H. Müller-Krumbhaar, *J. Cryst. Growth*, 1977, **42**, 11–14.
- 3 R. L. Penn, J. F. Banfield, *Science*, 1998, **281**, 969–971.
- 4 H. L. Xu, W. Z. Wang, W. Zhu, L. Zhou, M. L. Ruan, *Cryst. Growth. Des.* 2007, **7**, 2720–2724.
- 5 J. P. Liu, X. T. Huang, Y. Y. Li, *Cryst. Growth. Des.*, 2006, **6**, 1690–1696.